

THE INFLUENCE OF LIGHTWEIGHT FUNCTIONAL AGGREGATES ON THE ACIDIFICATION DAMAGE IN THE EXTERNAL ANODE MORTAR DURING CATHODIC PROTECTION FOR REINFORCED CONCRETE

Wenhao Guo (1), Jie Hu (1), Yuwei Ma (2), Haoliang Huang (1), Jiangxiong Wei (1) and Qijun Yu (1)

(1) School of Materials Science and Engineering, South China University of Technology, Guangzhou 510640, Guangdong, China

(2) Guangzhou University - Tamkang University Joint Research Center for Engineering Structure Disaster Prevention and Control, Guangzhou University, Guangzhou 510006, Guangdong, China

Abstract

Impressed current cathodic protection (ICCP) is an effective corrosion protection and prevention technique for reinforced concrete structures served in chloride-contaminated environment. The acidification damage in the external anode mortar caused by the anodic reactions significantly influences the efficiency of ICCP for reinforced concrete. Therefore, improving the acidification resistance of the external anode mortar is of great importance for the successful application of ICCP treatment. In this study, a novel type of lightweight functional aggregates was proposed to mitigate the acidification damage in the external anode mortar. The influence of the prepared lightweight functional aggregates both on the electrochemical performance of the primary anode and morphology, mineral compositions and microstructure of the secondary mortar were investigated.

The results indicated that the lightweight aggregates efficiently mitigated the damage of MMO coating on the primary anode surface, thus maintaining the high stability and catalytic activity of the primary anode. Severe acidification damage happened in the mortar matrix within a distance of 300 μm from the primary anode; beyond this region, the acidification damage was mainly propagated along the interfacial transition zone around the aggregates. Because the lightweight functional aggregates maintained the high alkalinity in the secondary mortar, the acidification damage both in the vicinity of the primary anode and ITZ around aggregates was significantly halted. Therefore, the prepared lightweight functional aggregates can be potentially used for preparing the high performance external anode mortar, further improving the stability and efficiency of ICCP treatment and durability of reinforced concrete structures.

Keywords: Cathodic protection, External anode mortar, lightweight functional aggregates, acidification damage, reinforced concrete

1. INTRODUCTION

Impressed current cathodic protection (ICCP) is proved to be an effective corrosion mitigation and rehabilitation technique for reinforced concrete structures under chloride-contaminated environment [1, 2]. The basic theoretical principle for ICCP treatment is to negatively polarize the embedded reinforcement (generally more cathodic than -850 mV vs saturated calomel electrode (SCE) [3]), thus thermodynamically inhibiting the electrochemical reactions related to corrosion damage of the reinforcement.

During ICCP treatment, the following anodic reactions will occur mainly on the surface and vicinity of the primary anode [4-6]:



The above reactions consume OH^- ions in the vicinity of the primary anode, thus leading to a pH drop of mortar pore solution. After the pH drop of mortar pore solution, the stability of hydration products at the primary anode/secondary mortar interface is reduced due to the altered micro-environment. The above process is known as acidification damage caused by the applied external current. The acidification damage of the external anode mortar can lead to more porous microstructure [4] and reduced adhesion at the primary anode/secondary mortar interface [7, 8], and also reduce the catalytic activity and subsequently increase the potential of the primary anode [9]. Therefore, improving the acidification resistance of the external anode mortar is of great importance for the successful application of ICCP treatment.

The preparation and optimization of the external anode mortar were widely investigated for decades. However, the optimization of the external anode mortar was mainly focused on improving either its conductivity or mechanical properties [10, 11]. To our best knowledge, the improvement related to the acidification resistance of the external anode mortar was not reported. To this end, the objective of this present paper is to apply lightweight functional aggregates (LFA) to prepare the high performance external anode mortar and investigate their mitigation effect on the acidification damage of the external anode mortar during ICCP treatment.

2. EXPERIMENTAL

2.1 Materials

Ordinary Portland cement (PII 42.5, China Resources Cement Holdings Ltd) and local tap water were used to prepare the mortar specimens. Two types of aggregates were applied for the preparation of the external anode mortar: the lightweight functional aggregates (LFA) and ordinary aggregates (NA). Commercially available porous ceramsites within the particle size of 3.5-4.0 mm were used for the preparation of LFA, and ordinary quartz river sands in the same size range were used as NA. The chemical composition of Portland cement is presented in Table 1. The sample designations in this study are as follows: specimens NA-20, NA-30

and NA-40 were the reference mortar specimens prepared with ordinary river sands with the volume fraction of 20 vol. %, 30 vol. % and 40 vol. %, respectively; specimens LFA-20, LFA-30 and LFA-40 were the mortar specimens prepared with lightweight functional aggregates with the volume fraction of 20 vol. %, 30 vol. % and 40 vol. %, respectively.

Table 1: Chemical composition of P II 42.5 Portland cement used in this study (wt. %)

Composition	SiO ₂	Al ₂ O ₃	Fe ₂ O ₃	CaO	MgO	K ₂ O	Na ₂ O	SO ₃	TiO ₂	LOI
Content	21.86	4.45	2.35	63.51	1.67	0.55	0.26	2.91	0.11	2.33

*LOI is the loss on ignition

Agar powders (C₁₂H₁₈O₉)_n used in this study were plant tissue culture grade with a gel strength of 1300 g/cm² (code: H8145). Analytical grade reagents (e.g. NaOH, Ca(OH)₂, KOH and NaCl) and deionized water were used for the preparation of LFA and simulated concrete pore solution. Carbon fibers used in this study were isotropic Polyacrylonitrile (PAN)-based series chopped carbon fibers (Jiangsu Elda Composite Material Co., Ltd).

The primary anode used in this study was mixed metal oxide (MMO) coated Ti wire (with a diameter of 2.0 mm and length of 60 mm). Q 235 construction steel reinforcement (with a diameter of 8 mm and length of 110 mm) was used as cathode. The working surface area of the reinforcement was 28.14 cm².

2.2 Sample preparation

(1) Preparation of the simulated concrete pore solution

In this study, simulated concrete pore solution was prepared based on the reported studies [12-14]: the concentration of Ca(OH)₂, NaOH and KOH was 0.002 mol/l, 0.06 mol/l and 0.18 mol/l, respectively; the pH of the simulated concrete pore solution was 13.29. Furthermore, 3 wt. % NaCl was added in the simulated concrete pore solution to simulate the chloride-contaminated environment.

(2) Preparation of the lightweight functional aggregates

The lightweight functional aggregates (LFA) were prepared by impregnating the modified agar gel solution into dry and preheated porous ceramics and the specific parameters and proportion of all components for the preparation of the modified agar gel solution are presented in Table 2. The impregnation procedure and related details for the preparation of LFA were similar to our previous study, and the resistivity of the prepared LFA was about 0.5 Ω·m [15].

Table 2: Mixture and preparation procedures of the modified agar solution in this study

Steps	Stirring speed (r/min)	Material added (wt. % per water weight)	Time (min)/Temp (°C)
1	30	Water/-- --	--/100.0
2	30	Agar powders/6.00	10.0/100.0
3	30	NaOH/0.33	0.5/90.0
4	30	KOH/1.40	0.5/90.0
5	60	Ca(OH) ₂ /8.62	1.0/90.0
6	120	Graphite powders/5.00	1.0/80.0~90.0

(3) Preparation of the external anode mortar specimen

In order to investigate the influence of the lightweight functional aggregates (LFA) on the acidification damage of the external anode mortar, cylindrical external anode mortar specimens with a height of 30 mm and diameter of 30 mm were prepared with the carbon fibers content of 0.75 vol. %. The volume fraction of aggregates (both NA and LFA) was 20 vol. %, 30 vol. % and 40 vol. %, respectively. MMO coated Ti wire (as the primary anode) with a length of 60 mm and diameter of 2 mm was placed in the axial center of the specimen, and the working surface area of the primary anode was 1.89 cm². The external anode specimens were cured at 20 ± 2 °C and 95 % relative humidity for 28 days before the accelerated acidification tests.

The positive and negative terminal of the external power supply (galvanostat, Corrtest CS1002) was connected to the primary MMO Ti anode and steel reinforcement, respectively. The surface area ratio of the secondary mortar and primary anode was 15:1. A constant current of 566 μA was applied, corresponding to a current density of about 200 mA/m² per surface area of the secondary mortar.

2.3 Methods

(1) Electrochemical measurements of the primary anode

Electrochemical impedance spectroscopy (EIS) and potentiodynamic polarization (PD) measurements were performed for the external anode mortar specimen before and after the accelerated acidification test. The specimen was depolarized for 24 h before the electrochemical measurements, and three-electrode system was used for all electrochemical measurements, in which the external anode mortar specimen was the working electrode (WE), saturated calomel electrode (SCE) was used as the reference electrode (RE) and Ti mesh with a surface area of 200 cm² was used as the counter electrode (CE). The frequency range for EIS measurement was 100 kHz-10 mHz, and the amplitude was ±10 mV vs. open circuit potential (OCP) of the primary anode. The scanning rate of potentiodynamic polarization was 0.5 mV/s in a potential range of -0.2 to 1.0 V vs. OCP of the primary anode.

(2) Optical fluorescence microscopy observation (OFM)

In order to investigate the acidification damage in the secondary anode mortar, the cross section of the external anode mortar specimen was observed by using optical fluorescence microscopy (OFM, Zeiss Discovery V12) with a excitation wavelength of 590 nm and magnifications range of 20× to 50×. After the accelerated acidification test, the cross section was cut from the middle part of the external anode mortar specimen and dried in vacuum oven at 40 °C until the weight of the cross section maintained constant. The fluorescent dye-containing epoxy (EpoFix pack, Struers Ltd) was then vacuum impregnated into the cross section specimen. The impregnated cross section specimen was polished with no.220, no.320, no.500, no.800, no.1200, no.2000 and no.3000 grinding papers, respectively.

(3) SEM observation

Scanning electron microscopy (SEM, EVO 18, Germany) was applied to investigate the morphology alterations at the primary anode/secondary mortar interface after the accelerated acidification test. SEM images with backscattered electron (BSE) mode were obtained for the

cross section specimen with an accelerating voltage of 20 kV and magnifications of 100× and 500×.

3. RESULTS AND DISCUSSIONS

3.1 The influence of LFA on the electrochemical performance of the primary anode

(1) Potential-dynamic polarization of the primary anode

The potentiodynamic (PD) polarization curves for all specimens after the accelerated acidification test are shown in Fig.1. It was observed that after the accelerated acidification test, the anodic current density for specimen LFA was higher than specimen NA with the same aggregates content when the same polarization potential was applied. Furthermore, a lower polarization potential was needed to obtain an anodic current density of 400 mA/m² (per surface area of the primary anode) which was normally used for ICCP treatment [2, 3, 5]. For example, the potential for obtaining the above anodic current density was 728 mV for specimen LFA and 1105 mV for specimen NA with the aggregate content of 40 vol. %, respectively. The above results confirmed that the lightweight functional aggregates were beneficial for maintaining the high catalytic activity and stability of the primary anode embedded in the external anode mortar.

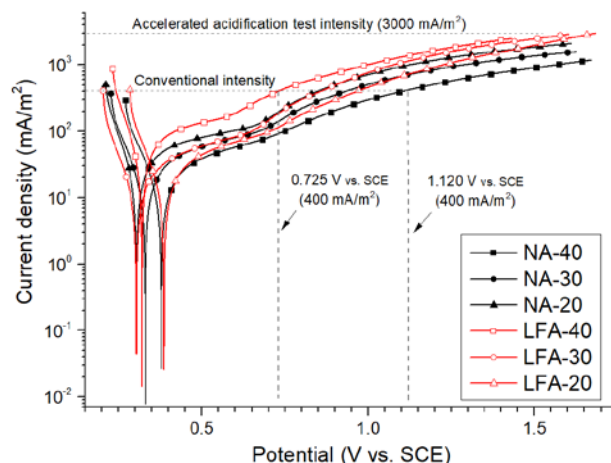


Figure 1: Potentio-dynamic (PD) polarization curves of all specimens after the accelerated acidification test

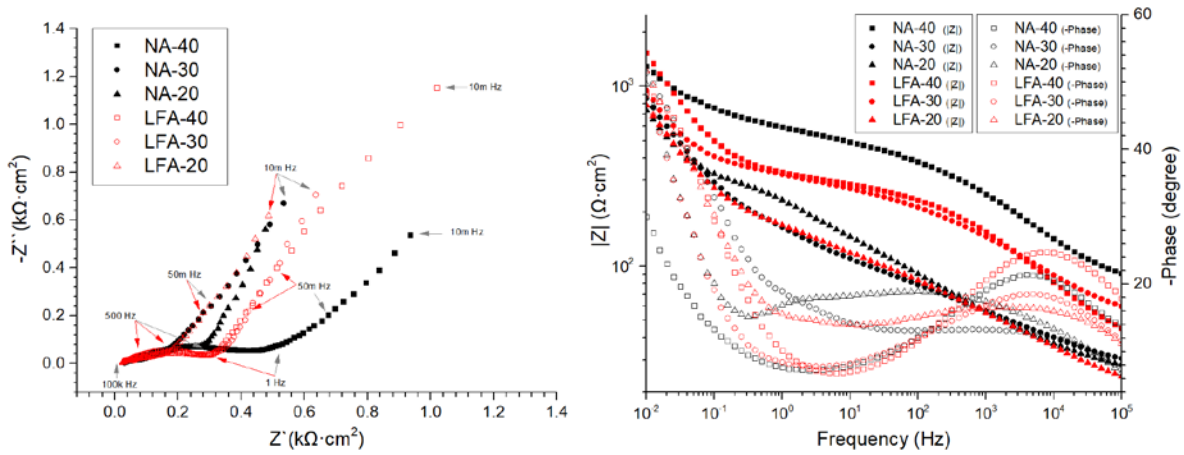
(2) The impedance response of the primary anode embedded in the external anode mortar

Fig.2 presents the impedance response of the specimens before and after the accelerated acidification test. In this study, EIS response was fitted by the equivalent circuit ($R_s((R_{ct}Z_w)Q_{dl})$) in this study. The physical meanings of the elements in the above equivalent circuit were as follows: R_s was the mortar matrix resistance, including the electrolyte resistance; R_{ct} was the charge transfer resistance of the primary anode, which represented the catalytic activity of MMO Ti anode for oxygen evolution; Q_{dl} was related to the property of the electrical double layer; Z_w was Warburg impedance.

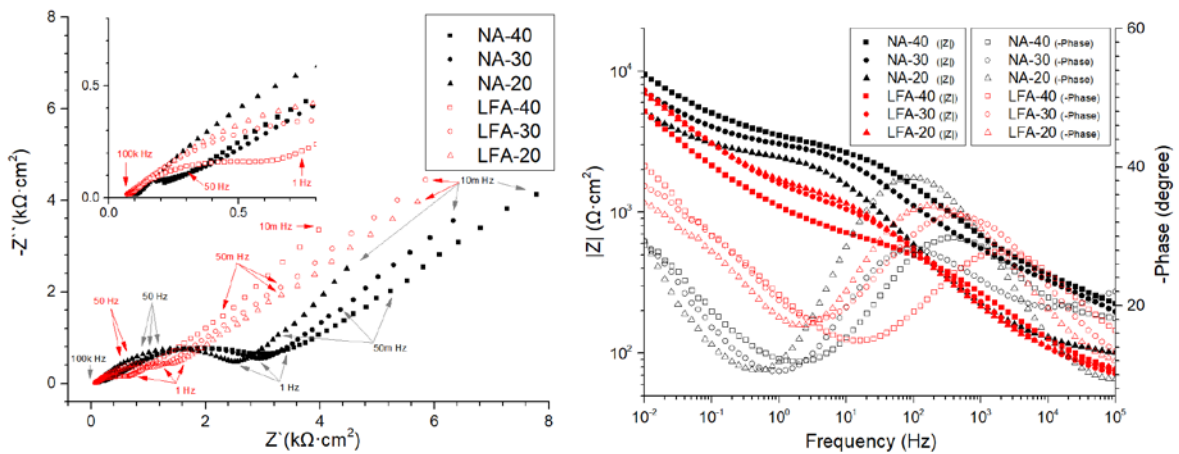
The derived mortar resistance (R_s) and Warburg impedance (Z_w) of different specimens are shown in Fig.3. It was observed in Fig.3 (a) that before the accelerated acidification test, the mortar resistance for all specimens was at the similar level. After the accelerated

acidification test, R_s for specimen NA was significantly increased. When the lightweight functional aggregates were used, R_s for specimen LFA was also increased; however, specimen LFA presented lower R_s value, compared to specimen NA. The lower R_s for specimen LFA was mainly attributed to the mitigation effect of the lightweight functional aggregates on the acidification damage of mortar matrix at the primary anode/secondary mortar interface, leading to a better adhesion between mortar matrix and carbon fibers/LFA and subsequently higher conductivity of the external anode mortar. It was also observed from Fig.3 (b) that Z_w of all specimens was dramatically reduced after the accelerated acidification test.

Fig.4 presents the derived charge transfer resistance (R_{ct}) and related electrical double layer capacitance (Q_{dl}) of different specimens. All the specimens presented very low R_{ct} and high Q_{dl} before the accelerated acidification test, indicating the good catalytic activity of the primary anode. After the accelerated acidification test, R_{ct} of all specimens increased and the related Q_{dl} was slightly reduced. The beneficial effect of the lightweight functional aggregates was evidenced by the lower R_{ct} of specimen LFA compared to specimen NA, indicating a better catalytic activity of specimen LFA after the accelerated acidification test.



(a) Before the accelerated acidification test



(b) After the accelerated acidification test

Figure 2: EIS responses in Nyquist and Bode format for the specimens before and after the AAT

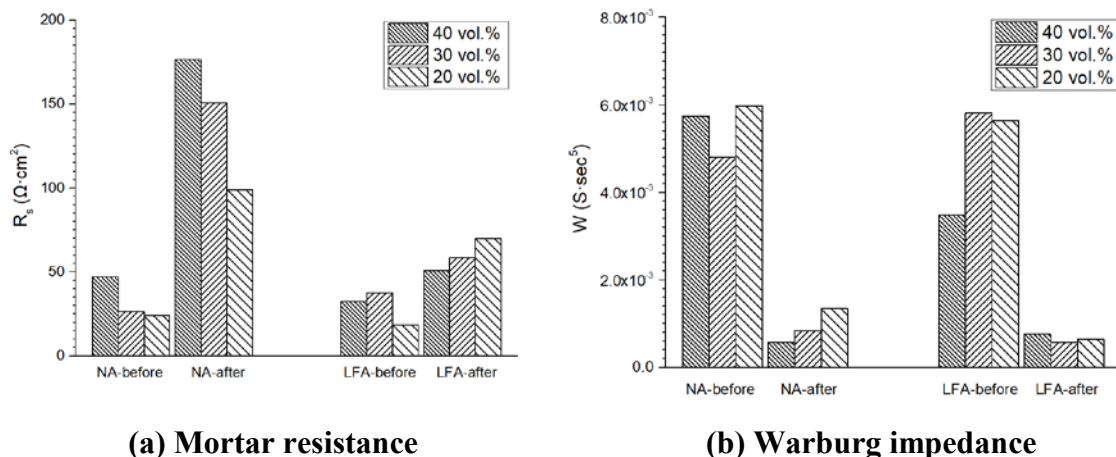


Figure 3: The derived mortar resistance (R_s) and Warburg impedance (Z_w) for different specimens before and after the accelerated acidification test

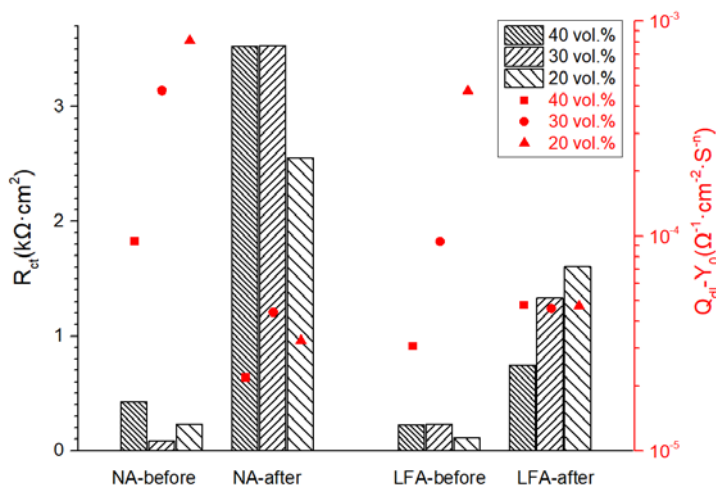
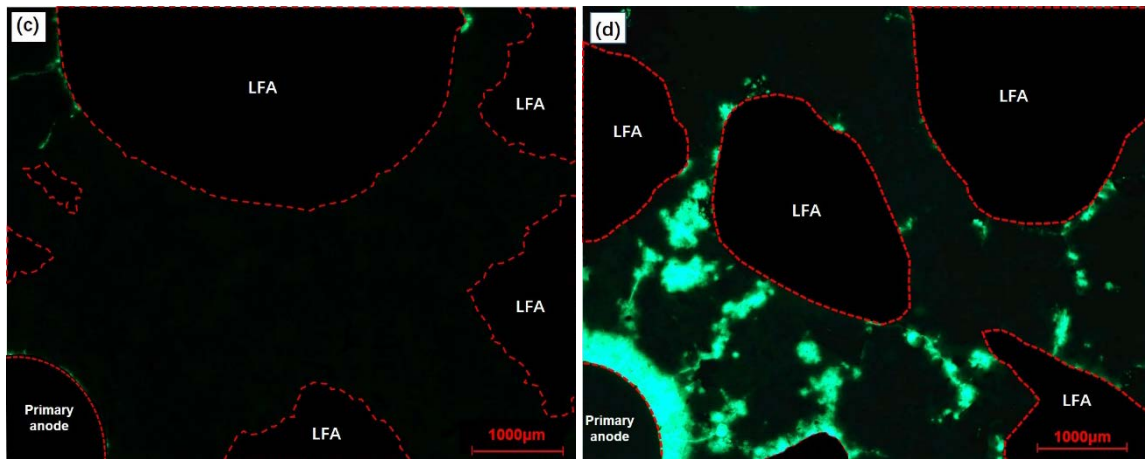


Figure 4: The derived charge transfer resistance (R_{ct}) and related electrical double layer capacitance (Q_{dl}) of different specimens before and after the accelerated acidification test

3.2 The influence of LFA on the acidification damage in the secondary mortar

(1) Acidification damage regions in the external anode mortar

The fluorescence microscopy images for specimens with 40 vol. % NA/LFA before and after the accelerated acidification test are shown in Fig.5.



(a) Specimen LFA before AAT

(b) Specimen LFA after AAT

Figure 5: The fluorescence microscopy images for specimen with an aggregate content of 40 vol. % NA/LFA before and after the accelerated acidification test (AAT)

After the accelerated acidification test, the acidification damage of the secondary mortar can be divided into two different regions. The first region was within the distance of about 300 μm from the primary anode surface. The most severe acidification damage happened in the vicinity of the primary anode, leading to porous microstructure in this region. Therefore, this region presented very bright colour in the fluorescence microscopy images. In this region, no obvious effect of the lightweight functional aggregates was observed, evidenced by the similar thickness of this region in the fluorescence microscopy images. Beyond the distance of about 300 μm from the primary anode surface, the acidification damage mainly occurred around the aggregate/mortar matrix interfacial transition zone (ITZ) and resulted in cracks in the mortar matrix. In this region, the lightweight functional aggregates halted the further propagation of the acidification damage, evidenced by the denser microstructure in ITZ and less cracks in the mortar matrix.

(2) Acidification damage in the vicinity of the primary anode

Fig.6 presents SEM images at the primary anode/secondary mortar interface for specimens with 40 vol. % NA/LFA after the accelerated acidification test. Two distinct acidification damage regions were also observed in SEM images, which was consistent with the fluorescence microscopy results. Compared to specimen NA, specimen LFA presented a denser microstructure in the severe acidification damage region (within a distance of 300 μm from the primary anode); furthermore, the cracks in the mortar matrix were also significantly less for specimen LFA. The above results indicated that the acidification damage degree in the external anode mortar was reduced by the lightweight functional aggregates.

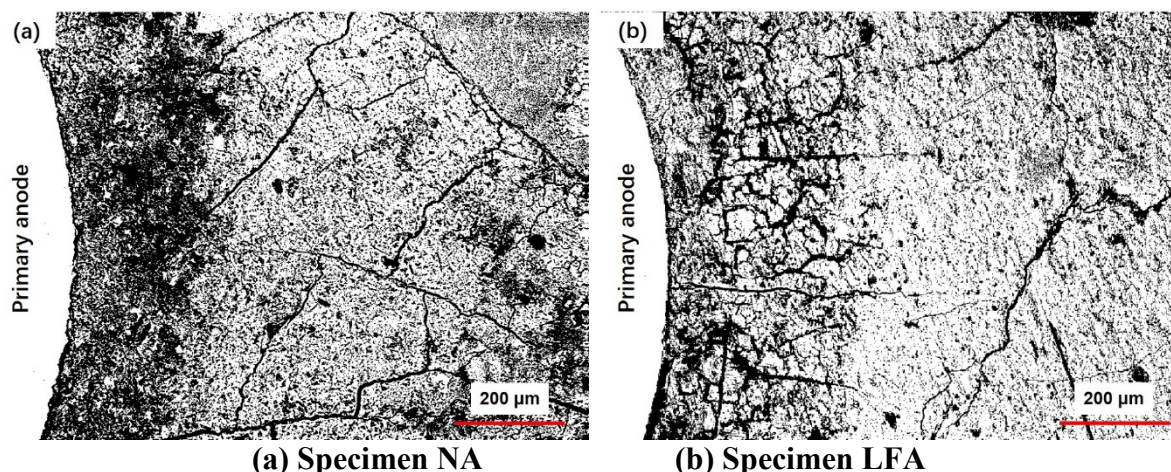


Figure 6: SEM images at the primary anode/secondary mortar interface after the accelerated acidification test: (a) specimen NA with the aggregate content of 40 vol. %; (b) specimen LFA with the aggregate content of 40 vol. %

(3) Acidification damage in the vicinity of the primary anode

SEM images and EDS analysis results in the vicinity of the aggregates with a distance larger than 1000 μm from the primary anode are shown in Fig.7. It was observed that specimen LFA presented a denser ITZ, compared to specimen NA; Ca/Si ratio in ITZ was significantly higher for specimen LFA (in the range of 0.58-1.64 for specimen NA and 1.97-4.82 for specimen LFA). The acidification damage area was also reduced by the lightweight functional aggregates, evidenced by the denser microstructure in the region with a distance larger than 50 μm from the aggregate. In this region, the difference in Ca/Si ratio of mortar matrix was small; however, specimen LFA still presented slightly higher Ca/Si ratio (in the range of 1.83-2.44), compared to specimen NA (1.74-2.28).

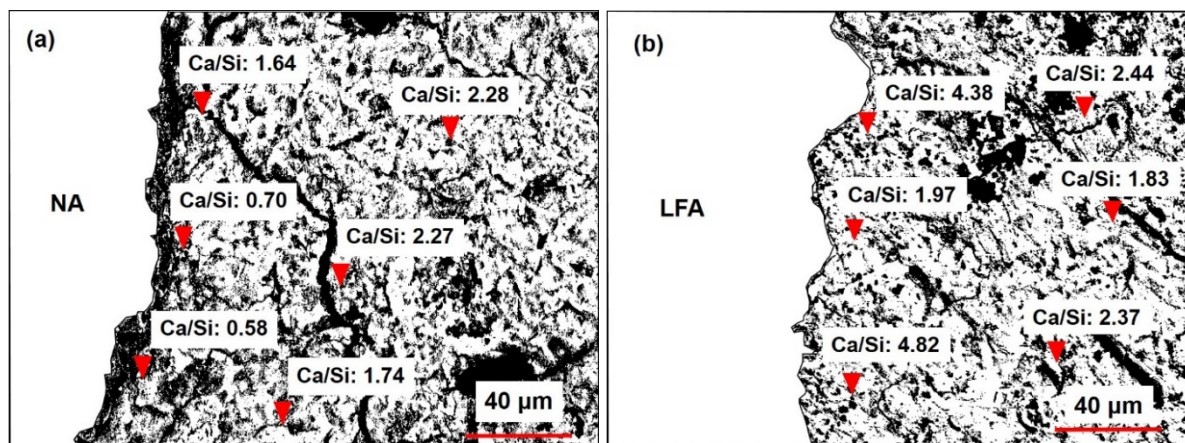


Figure 7: SEM images and EDS analysis results in the vicinity of the aggregates with a distance larger than 1000 μm from the primary anode after the accelerated acidification test: (a) specimen NA with the aggregate content of 40 vol. %; (b) specimen LFA with the aggregate content of 40 vol. %

4. CONCLUSIONS

In this study, a novel type of the external anode mortar was design and prepared based on lightweight functional aggregates and the influence of the lightweight functional aggregates on the acidification damage resulted from the applied external current during ICCP treatment was investigated. Based on the experimental results, the main conclusions in this study are summarized as follows:

(1) The lightweight aggregates efficiently mitigated the damage of MMO coating, thus maintaining the high stability and catalytic activity of the primary anode, e.g. lower anodic potential and charge transfer resistance of the primary anode.

(2) In this study, severe acidification damage happened in the mortar matrix within a distance of 300 μm from the primary anode; beyond this region, the acidification damage was mainly propagated around the interfacial transition zone around the aggregates.

(3) Because the lightweight aggregates maintained the high alkalinity in the secondary mortar by release OH^- from the aggregates, the acidification damage both in the vicinity of the primary anode and ITZ around aggregates was significantly halted. Therefore, the external anode based on the prepared lightweight functional aggregates presented excellent durability during ICCP treatment under chloride-contaminated environment.

ACKNOWLEDGEMENTS

This work was financially supported by Key Research and Development Program of China (Project No.2017YFB0309904), National Natural Science Foundation of China (No. 51572088, and 51602050), Pearl River S&T Nova Program of Guangzhou (No. 201806010188) and State Key Laboratory of Silicate Materials for Architectures (Wuhan University of Technology, No. SYSJJ2017-05). Their financial supports are gratefully acknowledged.

REFERENCES

- [1] US Federal Highway Administration, Memorandum on FHWA Position on Cathodic protection System in, 1982.
- [2] P. Pedeferra, Cathodic protection and cathodic prevention, *Construction and Building Materials*, 10 (1996) 391-402.
- [3] EN12696:2016, Cathodic protection of steel in atmospherically exposed concrete, European Committee for Standardization, 2016.
- [4] C.J. Weale, Cathodic Protection of Reinforced Concrete: Anodic process in cements and related electrolytes, in, Aston University, 1992, pp. 40-41.
- [5] J.P. Broomfield, Corrosion of steel in concrete: understanding, investigation and repair, 2nd ed., Taylor & Francis, London and New York, 1997, pp. 142-153.
- [6] J.E. Bennett, J.J. Bartholomew, J.B. Bushman, K.C. Clear, R.N. Kamp, W.J. Swiat, Cathodic Protection of Concrete Bridges: A Manual of Practice, in, Strategic Highway Research Program National Academy of Science, Washington, DC, 1993.
- [7] C.L. Page, G. Sergi, Development in cathodic protection applied to reinforced concrete, *Journal of Materials in Civil Engineering* 12 (2000) 8-15.
- [8] K. Wilson, M. Jawed, V. Ngala, The selection and use of cathodic protection systems for the repair of reinforced concrete structures, *Construction and Building Materials*, 39 (2013) 19-25.
- [9] S.D. Cramer, B.S. Covino, G.R. Holcomb, S.J. Bullard, W.K. Collins, R.D. Govier, R.D. Wilson, H.M. Laylor, Thermal sprayed titanium anode for cathodic protection of reinforced concrete bridges, *Journal of Thermal Spray Technology*, 8 (1999) 133-145.

- [10] X. Fu, D.D.L. Chung, Carbon fiber reinforced mortar as an electrical contact material for cathodic protection, *Cement and Concrete Research*, 25 (1995) 689-694.
- [11] S. Wen, D.D.L. Chung, Carbon fiber-reinforced cement as a thermistor, *Cement and Concrete Research*, 29 (1999) 961-965.
- [12] K. Andersson, B. Allard, M. Bengtsson, B. Magnusson, Chemical composition of cement pore solutions, *Cement and Concrete Research*, 19 (1989) 327-332.
- [13] Leemann, B. Lothenbach, C. Thalmann, Influence of superplasticizers on pore solution composition and on expansion of concrete due to alkali-silica reaction, *Construction and Building Materials*, 25 (2011) 344-350.
- [14] F. Puertas, A. Fernández-Jiménez, M.T. Blanco-Varela, Pore solution in alkali-activated slag cement pastes. Relation to the composition and structure of calcium silicate hydrate, *Cement and Concrete Research*, 34 (2004) 139-148.
- [15] W. Guo, J. Hu, Y. Wang, Z. Zhang, S. Yin, J. Wei, Q. Yu, Preparation and performance of conductive mortar based on lightweight conductive aggregates, *Construction and Building Materials*, 156 (2017) 340-350.